6184 Reprinted from Macromolecules, 1993, 26.

Elastic Properties of Polymer Films. 1. Elastic Constants of a Polyimide Film Determined by Brillouin Scattering and Mechanical Techniques

Sudha S. Kumar, A. Fartash,† and M. Grimsditch

Materials Science Division, Argonne National Laboratory, Argonne, Illinois 60439

Ivan K. Schuller

Department of Physics, University of California at San Diego, La Jolla, California 92093-0319

R. Sai Kumar*

New Products Research & Development, Amoco Chemical Company, Amoco Research Center, Naperville, Illinois 60566

Received April 12, 1993; Revised Manuscript Received August 6, 1993®

ABSTRACT: We discuss here the complete determination of the elastic properties of polymeric films using two experimental techniques. One technique employs the polymer film as a vibrating membrane and allows a direct determination of the "macroscopic" biaxial modulus, which serves as a figure of merit of polymer performance in applications such as packaging. Brillouin scattering, which measures the elastic properties on a ~100-μm scale, allows for a complete characterization of the elastic behavior. Both techniques have been applied to polyimide films. The results obtained by the two techniques are in agreement within the reported error bars.

Introduction

Plastic films have diverse applications such as food packaging, electronic packaging, thermal insulation, and membranes in filtering processes. Thermal and mechanical characteristics of a polymeric film usually dictate its level of performance in a given application. Mechanical properties of interest are usually stiffness, strength, toughness, and creep. Properties such as impact and tear resistance of polymeric films cannot easily be related to material characteristics such as molecular structure and organization since processing history, testing conditions, sample imperfections, and specimen geometry strongly influence these failure-related properties. The lack of correlation of these complex failure properties with the chemical and physical structure of the polymer precludes reliable experiments leading to formulation of theoretical models which allow useful prediction of structure–property relationships. Moreover, the usual testing procedures leading to measurements of toughness and strength of polymeric films are usually destructive by nature.

Stiffness, on the other hand, is a much simpler property to understand since it measures the resistance of a material to deformation. It is constitutive in nature and can be correlated with the structure of the material. Stiffness describes the elastic behavior of materials in the small strain region. As an extension of Hooke's law, the most general definition of "stiffness" is through either the elastic stiffness constants (C_{ij}) or the elastic compliance constants (S_{ij}). Although the C_{ij} and S_{ij} tensors are in reality fourth rank tensors with four indices, each index varying from 1 to 3, it is convenient to use the contracted notation where only two subindices are needed, with each index running from 1 to 6. It should be remembered however that in the contracted notation C_{ij} and S_{ij} are not tensors. In this notation the stress (σ) and strain (ϵ) are related through

$$\sigma_i = \sum C_{ij}\epsilon_j \quad \text{or} \quad \epsilon_i = \sum S_{ij}\sigma_j \tag{1}$$

In many cases it is useful to define simpler relationships such as the bulk modulus, Young's modulus, Poisson's ratio, etc. As will be discussed below, these are special cases of eq 1, and each one of these moduli can be expressed as a combination of C_{ij} or S_{ij} (see the appendix). In the most general case of a triclinic crystal the C_{ij} (or S_{ij}) array (which is symmetric in i and j) will have 21 independent components, whereas in the simplest case of an isotropic material, it only has two.

When dealing with single crystalline materials, the form of the C_{ij} array, and hence the number of independent components, is fixed by the crystal symmetry. The situation is not always so clear with semicrystalline polymers (i.e., contain some amorphous regions), for they usually are polycrystalline (i.e., contain many different crystalline grains) as well. Consequently the expected symmetry of the C_{ij} array may not be known a priori, being dependent on possible preferential molecular orientations brought about by various processing techniques. For example, if the molecules are randomly oriented, the material must be elastically isotropic and only two C_{ij} are needed to describe the system. Greater degrees of molecular orientation will require larger numbers of independent C_{ij}'s. The evaluation of the number of C_{ij} and their measurement for the particular case of Kapton, a commercial polyimide, is the subject of this investigation.

The experimental methods commonly used to obtain elastic constants can roughly be classified as follows: (i) macroscopic (static) stress–strain measurements, (ii) macroscopic dynamic mechanical methods, (iii) ultrasonic methods, and (iv) Brillouin scattering. If the sample consists of more than one structural domain, differences can be encountered in the measured value of a particular elastic constant, depending upon whether the test method is macroscopic (averages over many domains) or microscopic (measures a single domain). Differences may exist

† Present address: Texas Center for Superconductivity, Houston Science Center, University of Houston, Houston, TX 77204-5932.

® Abstract published in *Advance ACS Abstracts*, October 1, 1993.

0024-9297/93/2226-6184$04.00/0

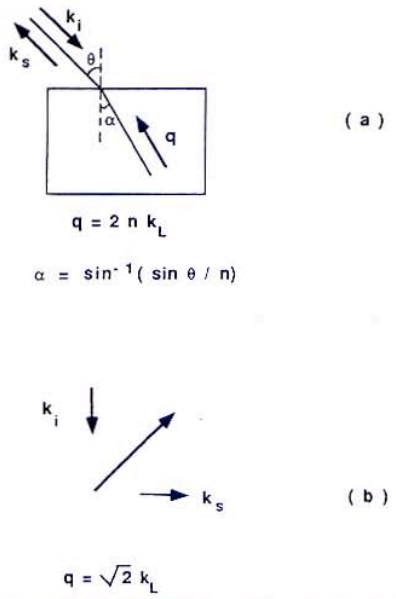

Figure 1. Scattering geometries used in Brillouin scattering experiments: back scattering (a) and platelet (b). $\mathbf{k}_i$, $\mathbf{k}_s$, and $\mathbf{q}$ are the incident, scattered, and phonon wave vectors, respectively. The scattering angle α is defined in the diagram and $k_L = 2\pi/\lambda$ where λ is the wavelength of the laser radiation.

due to the frequencies of the techniques, which become particularly important in viscoelastic media. For thin film polymers ultrasonic methods are very hard to apply and are almost never used. In such cases it is necessary to resort to less conventional techniques such as Brillouin scattering, and as a result, a complete determination of the elastic tensor is not always possible.

Brillouin scattering is not a novel technique in polymer science, and many review articles have discussed the usefulness of the technique in this field.[1-3] Brillouin scattering research with polymers has primarily been concerned with characterization of dynamics (segmental motion, relaxation, etc.) in the glassy state although the technique has been employed to measure the in-plane elastic properties of stretch-oriented polymers.[4-6]

We also describe in this paper a novel experimental technique for the direct measurement of the biaxial modulus of the polyimide film. Direct measurement of the biaxial modulus of polymeric films affords establishment of a figure of merit reflecting the performance of the polymer in packaging and/or membrane applications. Reliable comparisons across a set of materials can be made, allowing the best choice of high-performance materials for a given application.

Experimental Section

Brillouin scattering, the inelastic scattering of light by sound waves in a material, measures the velocity (and, in principle, the attenuation) of hypersonic thermal acoustic phonons. Because extensive theoretical and experimental reviews on Brillouin scattering techniques exist,[7] only a brief outline will be given here. The Brillouin scattering apparatus consists of an intense monochromatic source of well-collimated light (in this case a single-moded argon ion laser), a tandem Fabry–Perot interferometer to frequency analyze the scattered light, a detector, and a data acquisition system. The two scattering geometries used here are shown in Figure 1, denoted as backscattering (a) and platelet (b). In the backscattering geometry, phonons with wavevector $\mathbf{q} = 2nk_L$ (where n is the refractive index and k_L is the magnitude of the wavevector of the incident light) propagating close to the film normal can be probed. In the platelet geometry, phonons with $\mathbf{q} = \sqrt{2}k_L$ propagating in the plane of the film are investigated: a simple rotation about the surface normal allows selection of any direction in the film plane.

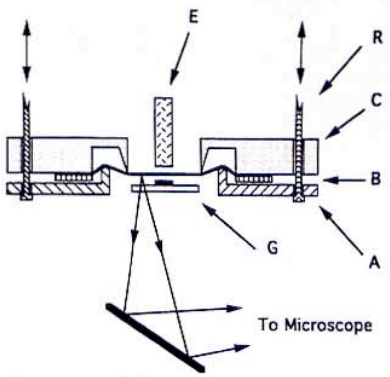

Figure 2. Schematic diagram of the apparatus used to measure the biaxial modulus.

The other experimental technique we used to measure the biaxial elastic modulus involves the determination of resonance frequencies of a radially (and isotropically) stretched circular membrane.[9] For films which are orders of magnitude thinner than their lateral dimensions elastic contributions are negligible and the resonant frequencies depend only on the applied tension.[8] Conversely, from the measured resonant frequencies the tension can be calculated. Since the strain in the film under tension can be measured with an optical microscope, the ratio of these two quantities yields the biaxial modulus. The biaxial modulus corresponds to the resistance to stretching in a plane rather than along a single direction as for Young's modulus.

A schematic diagram of the experimental cell is shown in Figure 2.[9] The cell consists of three main pieces: A, B, and C, which are assembled such that the film can be firmly mounted and stretched. Piece B clamps the film over a knife-edge on C that defines a circular boundary of $^3/_8$-in. diameter. Control of the tension is through the screws (R) that hold A in place. An electrode mounted on the reticule G generates an oscillating field that causes the film to vibrate. As the frequency of the voltage on the electrode is varied, the induced vibrational resonances are capacitively detected by a shielded electrode, E, facing the film. To minimize effects of hydrodynamic damping by air, the instrument is operated in vacuum ($<10^{-4}$ Torr). The strain (ϵ) was measured optically by viewing the film through a high magnification microscope. The rectangular reticule (G) positioned above the film allowed designated markings to be tracked as a function of tension, with a resolution of 0.5 μm. The ratio of radial stress to radial strain yields the biaxial modulus (E_b). Since the material has to be conductive for this method to be applicable, a thin (200-Å) layer of Al was evaporated onto the Type-H Kapton polyimide film (obtained from Du Pont Co., having a number-average molecular mass ranging between 20 000 and 25 000 g/mol[13]).

Theory

Before attempting to calculate the individual C_{ij} from experimental results, it is necessary to determine the nonzero elements and the number of independent elements in the C_{ij} array. Although the structure of Kapton has been reported to be either monoclinic or orthorhombic,[10] it is not clear what symmetry is to be expected for the elastic constant matrix, in the absence of information on preferential molecular orientation. It is therefore necessary to use other measured physical properties to determine its symmetry. One such property is the refractive index; since the material is birefringent in the plane of the film, the film normal can have at most 2-fold symmetry. Furthermore, if the film normal is structurally different from any in-plane axis, the symmetry of the C_{ij} array must be orthorhombic or lower, i.e., orthorhombic, monoclinic, or triclinic with 9, 13, or 21 independent C_{ij}, respectively.

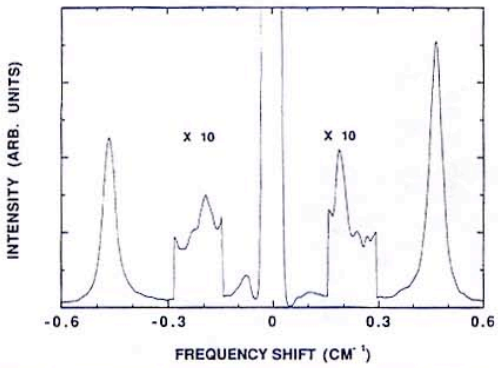

Figure 3. Brillouin spectrum of Kapton film in the backscattering geometry.

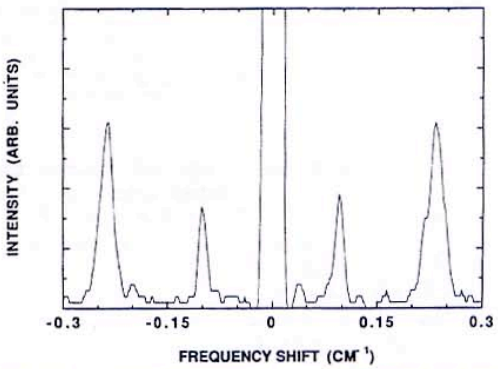

Figure 4. Brillouin spectrum of Kapton film in the platelet geometry.

Further narrowing down of the symmetry of Kapton requires some additional assumptions: if we assume that the orientation of the molecules does not distinguish between the top and bottom of the film, the symmetry cannot be triclinic. An equivalent assumption about any in-plane axis fixes the symmetry as orthorhombic. This is the symmetry we will take as a starting point for our investigation. The resulting C_{ij} array is given by

$$C_{ij} = \begin{pmatrix} C_{11} & C_{12} & C_{13} & 0 & 0 & 0 \\ C_{12} & C_{22} & C_{23} & 0 & 0 & 0 \\ C_{13} & C_{23} & C_{33} & 0 & 0 & 0 \\ 0 & 0 & 0 & C_{44} & 0 & 0 \\ 0 & 0 & 0 & 0 & C_{55} & 0 \\ 0 & 0 & 0 & 0 & 0 & C_{66} \end{pmatrix} \quad (2)$$

with its nine independent parameters. If this array is not sufficient to account for the measured results, some of the previous symmetry assumptions must be incorrect.

For the sake of completeness, we also present here the methodology for relating other elastic moduli to the C_{ij} array. Consider, for example, Young's modulus which is measured by applying a tension σ along a given direction (x in this example so that $\sigma_1 = \sigma$ and $\sigma_2 = \sigma_3 = \sigma_4 = \sigma_5 = \sigma_6 = 0$) and measuring its deformation (ϵ_1) along the same axis. It is clear from eqs 1 and 2 that $\epsilon_4 = \epsilon_5 = \epsilon_6 = 0$ and

$$\begin{aligned} \sigma &= C_{11}\epsilon_1 + C_{12}\epsilon_2 + C_{13}\epsilon_3 \\ 0 &= C_{12}\epsilon_1 + C_{22}\epsilon_2 + C_{23}\epsilon_3 \\ 0 &= C_{13}\epsilon_1 + C_{23}\epsilon_2 + C_{33}\epsilon_3 \end{aligned} \quad (3)$$

A solution of these three simulataneous equations yields ϵ_1 as a function of applied stress and the ratio: σ/ϵ_1 is Young's modulus (E_Y) along the x axis. The expression for E_Y resulting from eq 3 is long but easy to derive. Note, however, that, if the second half of eq 1 had been used instead, we would have obtained the equivalent but simpler expression

$$E_Y = 1/S_{11} \quad (4)$$

Equation 3 also directly leads to expressions for the generalized Poisson ratios defined as the ratio of the deformations perpendicular to and along the stress direction: ϵ_2/ϵ_1 and ϵ_3/ϵ_1. Similar derivations are easily made for other moduli and are discussed in the appendix.

Results

(i) Brillouin Scattering. Representative Brillouin spectra obtained in the backscattering and platelet geometries are shown in Figures 3 and 4, respectively. From the backscattering results such as those in Figure 3, we obtain the dependence of the Brillouin shift as a function of α (α is defined in Figure 1); the results are shown in Figure 5. We note that both the longitudinal (a) and transverse (b) modes exhibit an angular dependence, indicating that the film properties normal to the film are different from those in the plane. The platelet results, which reflect in-plane behavior, are shown in Figure 6. They show no clear evidence for any angular dependence in either the transverse or longitudinal Brillouin peaks. However, since the uncertainty of these experimental points is larger than that expected based on the accuracy for the peak positions, it may be an indication of inhomogeneities in the film on the order of the size of the laser spot, i.e., $\sim$100 μm.

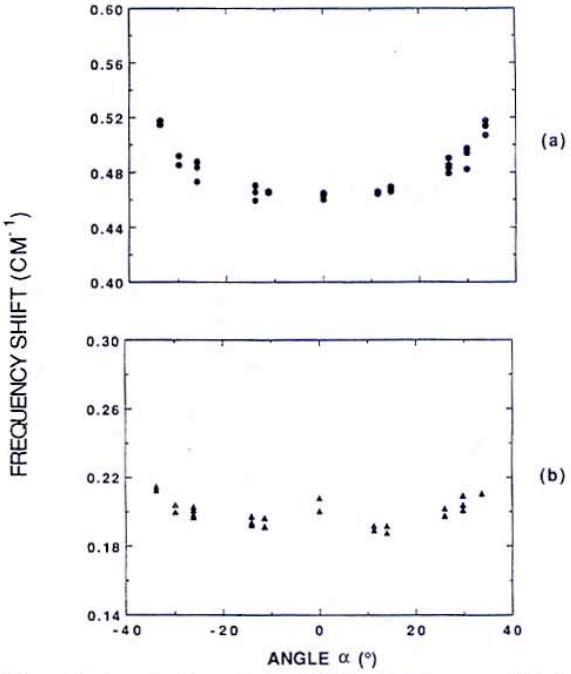

Figure 5. Angular dependence of Brillouin frequency shifts in the backscattering geometry: longitudinal (a) and transverse (b).

On the basis of the above data, we conclude, within our experimental accuracy, that Kapton exhibits isotropic behavior in the plane and anisotropic behavior out of the plane. Thus the polymeric film resembles a material with hexagonal symmetry in its elastic response. This measured symmetry is inconsistent with the orthorhombic symmetry presumed earlier; as such it must be considered to be an

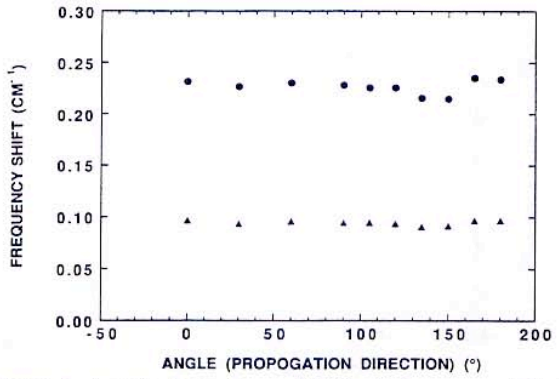

Figure 6. Angular dependence of Brillouin frequency shifts in the platelet geometry: longitudinal (dots) and transverse (triangles).

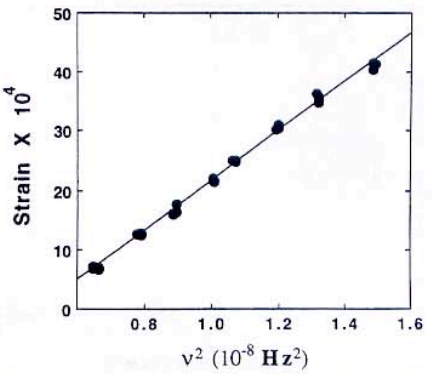

Figure 7. Strain versus the square of the fundamental frequency for Kapton film.

accidental degeneracy, or equivalently, that the accuracy of our measurements is not sufficient to resolve the in-plane anisotropy. With this indicated increased symmetry, defining the z axis to be the film normal, the C_{ij} array (eq 2) has the following additional restrictions: $C_{22} = C_{11}$, $C_{23} = C_{13}$, $C_{44} = C_{55}$, and $C_{66} = (C_{11} - C_{12})/2$ which reduces the number of independent parameters from 9 to 5. In other words, five independent elastic constants have to be determined to completely describe the elastic properties of the film.

These elastic constants can be determined from the Brillouin spectra acquired in different scattering geometries. The Brillouin frequency shifts are related to the velocities (v_q) of acoustic phonons by

$$\Delta\omega = 2n\omega_0(v_q/c)\sin(\theta/2)$$

where n is the refractive index, ω_0 the frequency of the incident light, c the velocity of light, and θ the scattering angle. The subscript q emphasizes that the velocity depends on the direction of propagation. Since the velocities along different directions are related to different C_{ij}'s, the latter are easily determined. In our data analysis we have used our measured value of n at 514 nm, viz., $n = 1.736 \pm 0.005$.

Thus from the backscattering geometry at $\alpha = 0$, C_{33} is obtained from the velocity of the longitudinal phonons and C_{44} from the velocity of the transverse phonons. Similarly from the in-plane longitudinal and transverse phonon velocities we can calculate C_{11} and C_{66}, respectively. C_{12} can be computed from $C_{66} = (C_{11} - C_{12})/2$. The remaining elastic constant C_{13} is obtained only indirectly from the angular dependence given in Figure 6 through a complex expression[11] which involves C_{11}, C_{33}, C_{44}, and α. This method of the determination of C_{13} is subjected to considerable error. Alternatively, C_{13} can be calculated from independently measured values of the biaxial modulus (E_b) and Young's modulus in-plane (E_Y), using expressions A.4 and A.2, respectively. The C_{ij} obtained from our Brillouin results are summarized in Table I. We note from Table I that C_{13} determined from different experimental techniques agree well within the experimental error bars shown. We stress again that these constants correspond to a material of hexagonal symmetry which is *higher* than expected. This should be taken to mean that our Brillouin results are not sensitive enough to detect an anisotropy which is known to be present because of the observed birefringence.

(ii) Biaxial Modulus. The normal modes (of vibration) of a film fixed on a circular boundary of radius a are well characterized.[8] The film behaves as a membrane when the restoring force is dominated by the tension T (force per unit area) applied to the film boundary. However, when the tension is negligible compared to the elastic stiffness of the film, it is treated as a plate, and its elastic response is different from that of a membrane. Whether a given material responds like a membrane or a plate depends on the ratio of its thickness to its diameter and also on its C_{ij}. Experimentally we found that our composite film (polymer + 200-Å aluminum) responds like a membrane, with the fundamental resonance (ν_{01}) given by

$$\nu_{01} = (0.38274/a)(T/\rho)^{1/2} \quad (5)$$

where ρ is the mass density. The higher resonances (ν_{ij}) are given by

$$\nu_{ij} = \beta_{ij}\nu_{01} \quad (6)$$

where i is the number of nodal lines and j is the number of nodal circles. β_{ij} are numbers; for the lowest modes they are $\beta_{11} = 1.5933$, $\beta_{21} = 2.1355$, and $\beta_{02} = 2.2954$.[8,9]

The measured strain versus the square of the resonant frequency is plotted for the polyimide film in Figure 7. Since ν^2 is a measure of the applied stress, Figure 7 basically depicts the stress–strain behavior of the polymeric film. The biaxial modulus therefore can be calculated from the slope of the straight line in Figure 7. Using the density 1.42 g/cm^3 for the polyimide film, we obtain a biaxial modulus of 5.26 ± 0.26 GPa (763 000 psi).

Discussion

For a material with hexagonal symmetry, and as found from the Brillouin measurements for Kapton, the expression for the biaxial modulus in terms of the C_{ij} is given by eq A.4. Using its measured value (5.26 ± 0.26 GPa), we obtain $C_{13} = 5.2 \pm 0.5$ GPa. Within our experimental error bars the elastic constants measured by Brillouin scattering and the mechanical technique are self-consistent. The expression relating the in-plane Young's modulus (E_Y^{in}) to the C_{ij} is given by eq A.2. Using the literature

Table I. Elastic Constants (GPa) of Kapton Film

	C_{11}	C_{33}	C_{13}	C_{12}	C_{44}	C_{66}
Brillouin scattering	8.9 ± 0.3	5.84 ± 0.12	5.6 ± 0.5	5.8 ± 0.3	1.2 ± 0.2	1.57 ± 0.03
mechanical technique			5.2 ± 0.5			
literature[12]			5.9 ± 0.2			

Table II. Elastic Moduli (GPa) of Kapton Film Calculated from the Elastic Constants Determined from Brillouin Scattering

	B	E_Y^{in}	E_Y^{out}	E_b	G_{in}	G_{out}
Brillouin scattering	5.8 ± 0.1	3.5 ± 1.0	1.6 ± 0.8	4.0 ± 2.0	1.57 ± 0.03	1.2 ± 0.2
mechanical technique				5.26 ± 0.26		
literature[12]		3.0 ± 0.3				

value[12] for E_Y^{in} (3 ± 0.3 GPa) and the Brillouin values of C_{11}, C_{12}, and C_{33} from Table I, we obtain C_{13} = 5.9 ± 0.2 GPa which is also in agreement with our measured values.

As remarked earlier, the elastic constants of a material provide fundamental information about the material characteristics. Knowledge of these constants helps us to completely and unequivocally describe the mechanical behavior of the material (under small strain). Many polymeric systems oriented in the form of fibers or films exhibit orthorhombic symmetry as indicated by wide-angle X-ray studies. Such systems need nine independent elastic constants to completely describe low-strain properties. Among these, C_{11}, C_{22}, and C_{33} represent extensional moduli; C_{12}, C_{13}, and C_{23} occur in expressions for Poisson's ratios; and C_{44}, C_{55}, and C_{66} represent shear deformations. For polymeric systems exhibiting hexagonal symmetry as in the case of the Kapton film investigated here, the actual number of independent elastic constants reduces to five, all of which have been determined above (see Table I).

Using the complete set of C_{ij} obtained from the Brillouin scattering experiments, we can calculate any particular modulus which relates to a particular deformation. Since within our experimental accuracy Kapton is hexagonal, we have summarized in the appendix expressions relating particular moduli to the C_{ij} in this case. In Table II we list the numerical values of these moduli which may be of interest in various applications.

Since our Brillouin spectroscopic measurements could not resolve the anisotropic elastic properties in the film plane, the maximum value of the elastic modulus measurable by conventional stress–strain testing is given by its tensile modulus, 3.0 GPa.[12] The higher measured biaxial modulus therefore indicates significantly enhanced stiffness in applications involving biaxial deformations than that indicated by macroscopic tensile test results. This conclusion is valid as long as the elastic response of the film remains Hookean (as evidenced by the linear stress–strain behavior). Thus we believe that direct measurement of the biaxial modulus by the technique given here provides a reliable means of predicting the performance of polymeric films in their most popular application: packaging.

Conclusions

Several high-performance polymeric materials are commonly fabricated in thin film forms. Certain polyimides, polyaramides, and polymers such as poly(benzobisthiazole), etc., are examples of polymers that are usually processed in the form of films. Irrespective of the nature of the system being investigated, we should keep in mind that polymer morphology plays a very important role in governing the thermomechanical properties. Thus any experimental technique that provides determination of properties through preservation of polymer morphology is desirable. In addition, we generally prefer experimental techniques involving minimal sample preparation. The Brillouin spectroscopic technique described here is nondestructive and allows a thorough characterization of the elastic properties of polymeric films. Since both the experimental techniques described here basically measure fundamental material constants, we should be able to establish structure–property relationships in a straightforward manner, through similar measurements on a number of polymeric systems.

Acknowledgment. We thank Kenneth McKenzie of Amoco Technology Corp. for his help in metal coating of Kapton polyimide film. We also appreciate Beverley Holze and Costas Metaxas for their help in measuring the refractive indices of Kapton. Work at Argonne National Laboratory was supported by the U.S. Department of Energy, Basic Energy Sciences and Materials Sciences, under Contract No. 31-109-ENG-38 and at the University of California at San Diego by ONR Grant No. N00014-91j-1438.

Appendix

In this appendix we define and derive expressions for various moduli of a material with hexagonal symmetry.

(i) Bulk modulus (B): relates the volume change (ΔV) to an applied hydrostatic pressure (P). In this case we have $-P = \sigma_{xx} = \sigma_{yy} = \sigma_{zz}$ and $\Delta V = \epsilon_{xx} + \epsilon_{yy} + \epsilon_{zz}$.

$$B = -P/\Delta V = (C_{11}C_{33} + C_{12}C_{33} - 2C_{13}^2)/(2C_{33} + C_{11} + C_{12} - 4C_{13}) \quad \text{(A.1)}$$

(ii) In-plane Young's modulus (E_Y^{in}): ratio of applied uniaxial in-plane stress (σ_{xx}) to in-plane strain (ϵ_{xx}).

$$E_Y^{in} = (C_{11} - C_{12})\{1 - (C_{13}^2 - C_{12}C_{33})/(C_{11}C_{33} - C_{13}^2)\} \quad \text{(A.2)}$$

(iii) Out-of-plane Young's modulus (E_Y^{out}): ratio of applied uniaxial out-of-plane stress (σ_{zz}) to out-of-plane strain (ϵ_{zz}).

$$E_Y^{out} = C_{33} - 2C_{13}^2/(C_{11} + C_{12}) \quad \text{(A.3)}$$

(iv) Biaxial modulus (E_b): ratio of applied biaxial in-plane stress ($\sigma_{xx} = \sigma_{yy}$) to biaxial in-plane strain ($\epsilon_{xx} - \epsilon_{yy}$).

$$E_b = C_{11} + C_{12} - 2C_{13}^2/C_{33} \quad \text{(A.4)}$$

(v) In-plane shear modulus: ratio of applied in-plane shear stress (σ_{xy}) to the in-plane shear strain (ϵ_{xy}).

$$G_{in} = \sigma_{x4}y/\epsilon_{xy} = C_{66} \quad \text{(A.5)}$$

(vi) Out-of-plane shear modulus: ratio of applied out-of-plane shear stress (σ_{xz}) to the out-of-plane shear strain (ϵ_{xz}).

$$G_{out} = \sigma_{xz}/\epsilon_{xz} = C_{44} \quad \text{(A.6)}$$

References and Notes

(1) Patterson, G. D. *Probing Polymer Structures*; Advances in Chemistry Series 174; American Chemical Society: Washington, DC, 1979; p 141.
(2) Patterson, G. D. *J. Polym. Sci., Macromol. Rev.* **1980**, *15*, 1.
(3) Patterson, G. D. *Methods Exp. Phys.* **1980**, *16A*, 170.
(4) Adamic, R. J.; Wang, C. H. *Macromolecules* **1984**, *17*, 2018.
(5) Liu, Q. L.; Wang, C. H. *Macromolecules* **1983**, *16*, 482.
(6) Cavanaugh, D. B.; Wang, C. H. *J. Appl. Phys.* **1982**, *53*, 2793.
(7) Sandercock, J. In *Festkorperprobleme*; Advances in Solid State Physics; Queisser, H. J., Ed.; Pergamon: New York, 1975; Volume XV, p 183.
(8) Morse, P. M. *Vibration and Sound*, 2nd ed.; McGraw-Hill: New York, 1948; p 172.

(9) Fartash, A.; Grimsditch, M.; Schuller, I. K. *Appl. Phys. Lett.* **1989**, *55*, 2614. Fartash, A.; Schuller, I. K.; Grimsditch, M. *Rev. Sci. Instrum.* **1991**, *62*, 494.
(10) (a) Sidorovich, A. V.; Baklagina, Yu. G.; Kenarov, A. V.; Nadezhin, Yu. S.; Adrova, N. A.; Florinski, F. S. *J. Polym. Sci., Polym. Symp.* **1977**, *58*, 359. (b) Conte, G.; D'Ilario, L.; Pavel, N. V.; Giglio, E. *J. Polym. Sci., Polym. Phys. Ed.* **1976**, *14*, 1553.
(11) Chiang, T. C. *Solid State Commun.* **1978**, *28*, 7.
(12) Product Literature, E. I. du Pont de Nemours and Co., 1987.
(13) Private communication with the technical service representative of the High Performance Films Division of Du Pont Co.